

Original Article

Cite this article: Müller SP, Kroh A, Birgel D, Goedert JL, Kiel S, and Peckmann J (2023) Mass occurrence of echinoids in an Oligocene hydrocarbon-seep limestone from the Olympic Peninsula, Washington State, USA. *Geological Magazine* 160: 941–954. <https://doi.org/10.1017/S0016756823000067>

Received: 20 September 2022

Revised: 20 December 2022

Accepted: 16 January 2023

First published online: 10 March 2023

Keywords:

Echinoidea; spatangoids; methanotrophic archaea; chemosynthesis; lipid biomarkers; Makah Formation

Author for correspondence: Jörn Peckmann,

Email: joern.peckmann@uni-hamburg.de

Mass occurrence of echinoids in an Oligocene hydrocarbon-seep limestone from the Olympic Peninsula, Washington State, USA

Sandro P Müller¹, Andreas Kroh² , Daniel Birgel¹, James L Goedert³, Steffen Kiel⁴ and Jörn Peckmann¹ 

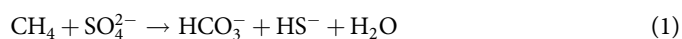
¹Center for Earth System Research and Sustainability, Institute for Geology, University of Hamburg, Hamburg 20146, Germany; ²Natural History Museum Vienna, Geological–Palaeontological Department, Vienna 1010, Austria; ³Burke Museum of Natural History and Culture, University of Washington, Seattle, WA 98195, USA and ⁴Department of Palaeobiology, Swedish Museum of Natural History, Stockholm 10405, Sweden

Abstract

Loose limestone blocks of a newly recognized hydrocarbon-seep deposit from the lower Oligocene Jansen Creek Member of the Makah Formation were collected on a beach terrace close to the mouth of Bullman Creek in Washington State, USA. The limestone consists largely of authigenic carbonate phases, including ¹³C-depleted fibrous cement forming banded and botryoidal crystal aggregates with $\delta^{13}\text{C}$ values as low as -23.5 ‰. Lipids extracted from the limestone yielded molecular fossils of anaerobic methanotrophic archaea (ANME), dominated by compounds of an ANME-2/DSS consortium with $\delta^{13}\text{C}$ values as low as -106 ‰, indicating formation at an ancient methane seep. The fossil inventory of the seep deposit is remarkable, consisting almost solely of echinoid remains, whereas typical seep biota are absent. Varying preservation of the echinoid fossils indicates parautochthonous deposition, corroborated by evidence for high fluid flow at the ancient seep, possibly responsible for displacement of echinoids after death. Although a full taxonomic description of the echinoids cannot be given, almost all fossils were assigned to one taxon of irregular spatangoids, except for a single regular echinoid. Abundance and lifestyle of the irregular spatangoids in the Bullman Creek echinoid seep deposit resemble those of the fossil *Tithonia oxfordiana* from an upper Jurassic seep deposit in France and extant *Sarsiaster griegii* from modern seeps in the Gulf of Mexico. The Bullman Creek echinoid deposit probably represents a fossil analogue of the Gulf of Mexico *Sarsiaster* mass occurrence, indicating that the adaptation of spatangoid echinoids to chemosynthesis-based ecosystems ranges back at least to the earliest Oligocene.

1. Introduction

Recent and ancient hydrocarbon-seep deposits can be found worldwide in different geological contexts of passive and active continental margins, where fluids rich in reduced components, mainly methane, are emitted (e.g. Paull *et al.* 1984; Sibuet & Olu, 1998; Campbell, 2006; Joye, 2020; Cochran *et al.* 2022). These fluids constitute the energy source of chemosynthesis-based ecosystems, characterized by high-abundance and low-diversity faunas typically dominated by bivalves and tubeworms (Peckmann & Thiel, 2004). At seeps, methane is consumed by a consortium of anaerobic methanotrophic archaea (ANME) and sulphate-reducing bacteria. This metabolism, referred to as sulphate-driven anaerobic oxidation of methane (AOM), constitutes the key biogeochemical process at seeps (Hinrichs *et al.* 1999; Thiel *et al.* 1999; Boetius *et al.* 2000; Peckmann & Thiel, 2004).



Release of bicarbonate and hydrogen sulphide from AOM favours the precipitation of authigenic carbonate and sulphide minerals (Ritger *et al.* 1987). Furthermore, hydrogen sulphide is utilized as an energy source by sulphide-oxidizing bacteria, including thiotrophs living as symbionts within different metazoan hosts like siboglinid tubeworms, solemyid, lucinid, thyasirid, vesicomyid and bathymodiolin bivalves (Sibuet & Olu, 1998; Dubilier *et al.* 2008). Seep limestones can be identified by the low $\delta^{13}\text{C}$ values of their early diagenetic carbonate phases, inheriting ¹³C depletion from parent methane (e.g. Peckmann & Thiel, 2004; Zwicker *et al.* 2015). However, the $\delta^{13}\text{C}$ values are typically not as negative as those of the original methane due to substantial incorporation of non-AOM-derived carbon, including marine dissolved inorganic carbon (e.g. Ritger *et al.* 1987; Campbell *et al.* 2002; Kiel & Peckmann, 2007). In addition to this isotopic signature, ancient seep deposits can be recognized by their paragenetic sequence, usually consisting of a micritic matrix, fibrous banded and botryoidal cements as well as equant

© The Author(s), 2023. Published by Cambridge University Press. This is an Open Access article, distributed under the terms of the Creative Commons Attribution licence (<http://creativecommons.org/licenses/by/4.0/>), which permits unrestricted re-use, distribution and reproduction, provided the original article is properly cited.



calcite cement, occasionally accompanied by authigenic quartz (e.g. Campbell *et al.* 2002; Kuechler *et al.* 2012; Smrzka *et al.* 2015; Hryniewicz, 2022a). At modern seeps fibrous cements almost exclusively consist of aragonite, whereas in ancient seep deposits aragonite is commonly recrystallized to calcite (Beauchamp & Savard 1992; Savard, 1996; Peckmann *et al.* 2001, 2002; Campbell *et al.* 2002).

In this study we investigated a seep limestone from the earliest Oligocene Jansen Creek Member of the Makah Formation in Washington State. In contrast to other ancient seep limestones typically dominated by bivalves, gastropods and worm tubes, the fauna of the new deposit consists almost exclusively of echinoids. This is peculiar because echinoderms, and especially echinoids, are rarely reported living at seeps (e.g. Carney, 2010; Pawson *et al.* 2015) or as fossils from ancient seeps (e.g. Kato *et al.* 2017; Brezina *et al.* 2022). We combine petrographical, geochemical and palaeontological analyses to shed light on the occurrence, taphonomy and preservation of echinoids at this ancient hydrocarbon-seep deposit and discuss possible adaptations of echinoids to chemosynthesis-based ecosystems.

1.a. Geological setting

The study site is located on the north coast of the Olympic Peninsula in western Washington State, USA, eastward of the accretionary wedge of the Cascadia subduction zone, where the Juan de Fuca Plate has been subducted beneath the North American Plate since the late Eocene (Fig. 1). The accretionary wedge is characterized by rapid burial as well as high pressure and sedimentation rates. Subduction causes sediment compaction resulting in excess pore pressure that forces water rich in compounds such as carbon dioxide and methane out of the strata. Structural deformation, permeable horizons and fault zones enable these fluids to move towards the seafloor where they can form the basis of chemosynthesis-based habitats such as hydrocarbon seeps (e.g. Ritger *et al.* 1987; Moore & Vrolijk 1992; Scholz *et al.* 2013). In western Washington State, numerous ancient hydrocarbon-seep sites have been described and range in age from the middle Eocene c. 42.5 to 40.5 Ma to the Mio-Pliocene c. 5 Ma (e.g. Goedert & Squires, 1990, 1993; Campbell, 1992; Peckmann *et al.* 2002, 2003, 2007; Goedert *et al.* 2003; Goedert & Peckmann, 2005; Kiel, 2006, 2010; Amano & Kiel, 2007; Nesbitt *et al.* 2013; Hybertsen & Kiel, 2018; Hryniewicz, 2022b). Most of the ancient hydrocarbon-seep sites occur within sediments overlying an early Eocene basalt basement, the so-called Coast Range Terrane (Snively & Wells, 1996; Fig. 1) or Siletzia (e.g. Wells *et al.* 2014). As noted by Jakubowicz *et al.* (2020), strata enclosing most of the reported Palaeogene seep deposits in Washington were deposited in retro-forearc basins associated with the Cascadia subduction zone and are not actually part of the uplifted accretionary wedge. Approximately 16 to 15 Ma ago, a shift in the geometry of the Cascadia subduction zone resulted in uplift of parts of Siletzia and the formation of the Olympic Mountains (Brandon & Vance, 1992; Brandon *et al.* 1998; Stewart & Brandon 2004). Due to this uplift, sediments that once filled the Tofino Basin, predominantly deep-water rocks of Eocene to late Oligocene age, now crop out along the north side of the Olympic Peninsula almost continuously for a distance of over 80 km (Tabor & Cady 1978; Snively *et al.* 1993). Within these strata, the Makah Formation comprises six members and a total thickness of c. 2800 m of siltstone and sandstone that were deposited on the fringes of a submarine fan at lower to middle bathyal depths (Snively *et al.* 1980).

The limestone studied herein, derived from the Jansen Creek Member of the Makah Formation, was collected on a beach terrace c. 1 km east of the mouth of the Bullman Creek (48.3466° N, 124.5204° W), Clallam County, Washington. The Makah Formation includes strata that range in age from the late Eocene (late Narizian, c. 36 Ma) to the early Oligocene (Zemorrian, c. 30 Ma; Snively *et al.* 1980; Prothero *et al.* 2009). The Jansen Creek Member is an olistostrome (Snively *et al.* 1980; Niem *et al.* 1989), c. 10 km long and 200 m thick, composed of uppermost Eocene and lowermost Oligocene fossiliferous sandstones (both deep- and shallow-water marine) and other clastics including shallow water conglomerate that slid off a shelf in the area that is now Vancouver Island (Snively *et al.* 1993) and into the deep Tofino Basin. It is not known if this submarine slide was a single event, or if the basin accumulated slump and slide debris over an extended period. The debris is enclosed stratigraphically below and above by slightly younger deep-water sand- or siltstones. Seep carbonates are common in the Jansen Creek Member. Goedert and Campbell (1995) described allochthonous seep carbonate in penecontemporaneously disturbed strata near Shipwreck Point, 6.8 km SE of the Bullman Creek site. Although Goedert and Campbell (1995) estimated the Shipwreck Point site to be stratigraphically 30 m above the Jansen Creek Member, based on mapping by Snively *et al.* (1993) it could be interpreted as being in the Jansen Creek Member. A turbidite deposit associated with the Jansen Creek Member contains vesicomid bivalves (Goedert & Squires, 1993), and a species of *Bathymodiolus* was found in seep limestone from the Jansen Creek Member (Kiel & Amano, 2013). Based on benthic foraminifers and macrofossil inventory, Goedert & Campbell (1995) proposed mid- to lower bathyal depths as the depositional environment for the seep deposit of the Makah Formation at Shipwreck Point. Burns and Mooi (2003) mentioned a regular echinoid resembling *Strongylocentrotus* from deep-water rocks of the Jansen Creek Member, but these are rare, were not found in hydrocarbon-seep deposits and have not been described yet. Squires (1995) reported gastropods, and Hryniewicz *et al.* (2017) reported thyasirid bivalves from other seep limestone located close to the Bullman Creek echinoid seep deposit reported here.

2. Materials and methods

All samples of the Bullman Creek echinoid seep deposit are archived in the Department of Palaeobiology, Swedish Museum of Natural History, Stockholm, Sweden, with the catalog number NRM Ec37156. Seven thin-sections of either 150 × 100 mm or 100 × 75 mm, prepared at the GeoZentrum, Erlangen, Bavaria, Germany, were studied. Parts of the thin-sections were stained with a mixture of potassium ferricyanide and alizarin red solution, dissolved in 0.1 % HCl (Dickson, 1966) and with Feigl's solution (Feigl, 1958). For petrographical analysis of the thin-sections, a Zeiss Axio Scope.A1 was used. Photographs were taken with a Canon EOS1300D digital camera. Photographs of echinoids were taken with the software ZENcore v.3.1 on a Zeiss Axio Vision V20 equipped with a Zeiss PlanAPO S ×0.63 objective and Zeiss AxioCam 712 colour camera.

Samples for stable isotope analysis ($\delta^{13}\text{C}$, $\delta^{18}\text{O}$) were obtained from the rock slabs from which thin-sections had been prepared, using a hand-held microdrill. Analyses were conducted at the Zentrum für Marine Umweltwissenschaften (MARUM), Universität Bremen, using a ThermoFisher ScientificTM 253plus gas isotope ratio mass spectrometer with Kiel IV automated

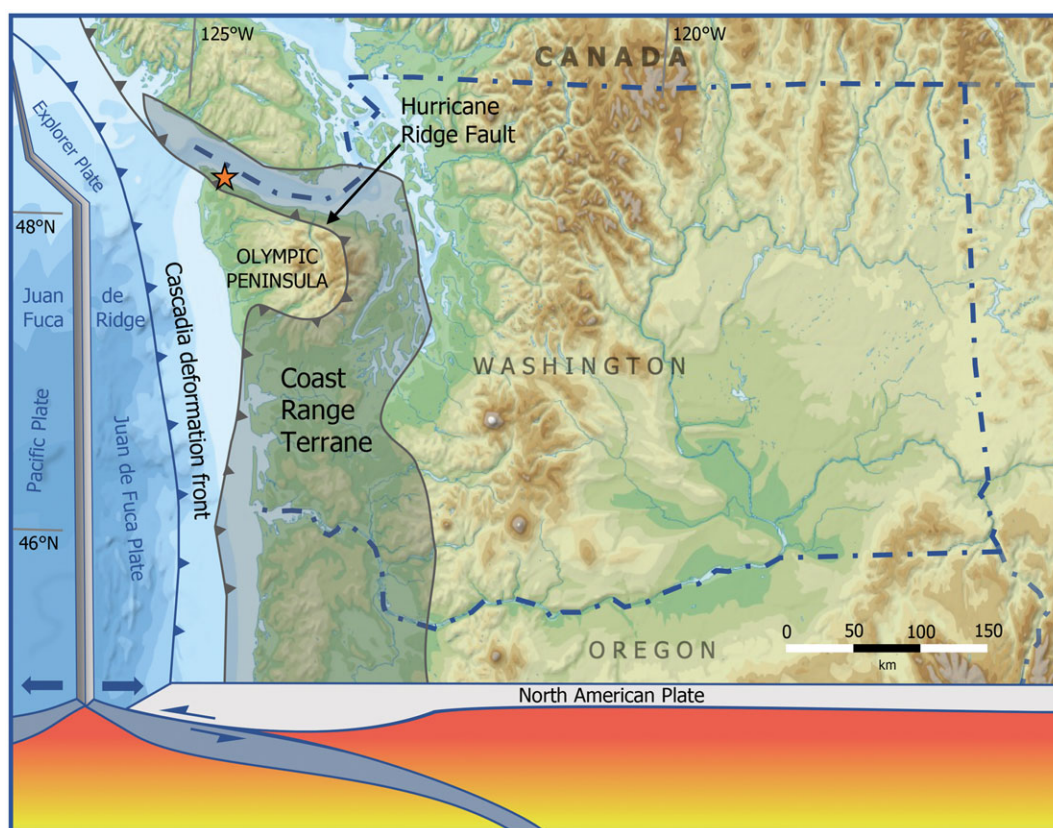


Fig. 1. (Colour online) Physical map of Washington State showing the Olympic Peninsula. The shaded area represents the Coast Range Terrane. Star marks the Bullman Creek echinoid seep deposit. At the bottom of the image the subduction of the Juan de Fuca Plate beneath North America as well as the Juan de Fuca Ridge are illustrated. Base map of Washington State modified after Wikimedia Commons User: Bourrichon. Coast Range Terrane and Hurricane Ridge Fault redrawn from Stewart & Brandon (2004).

carbonate precipitation device. Upper Jurassic Solnhofen limestone was used as in-house standard; standard deviations of $\delta^{13}\text{C}$ and $\delta^{18}\text{O}$ values were 0.02 ‰ and 0.05 ‰, respectively. All isotope ratios are reported relative to the Vienna Pee Dee Belemnite (VPDB) standard.

One limestone sample was prepared for analysis of molecular fossils, following the procedure of Birgel *et al.* (2006b). The limestone sample (193 g) was crushed to small pieces and cleaned with acetone. To release molecular fossils preserved in the carbonate lattice, 10 % HCl was carefully poured upon the sample until about two-thirds of the carbonate was dissolved. After dissolution, four standards were added: 5 α -(H)-cholestane, 1-nonadecanol, C₁₈/C₁₈-dialkyl glycerol diether and 2-methyl-octadecanoic acid. Then, 6 % KOH in methanol was added for alkaline hydrolysis to release bound fatty acids from the carbonate matrix by ultrasonication at 80 °C for two hours. After saponification, the sample was centrifuged at 2500 rpm, and the supernatants (i.e. alkaline hydrolysis extract) were decanted and collected in a separatory funnel. Extraction of molecular fossils was done by ultrasonication (15 min at ambient temperature) with dichloromethane/methanol (3:1) and centrifuged afterwards (2500 rpm). Extraction was repeated four times until the solvents became colourless; the extracts were combined with the alkaline hydrolysis extract. After the extractions, water was added to separate the organic phase from the aqueous phase. The fatty acids were released from the aqueous into the organic phase by acidification with 10 % HCl to pH 1–2. The resulting total lipid extract was further separated into maltenes and asphaltenes. The latter fraction contained highly

polar and complex macromolecules, which were not further analysed. The maltene fraction contained easy extractable compounds and was separated by solid phase column chromatography (NH₂-propyl modified silica gel, 500 mg; Macherey-Nagel) into four fractions of increasing polarity (hydrocarbons, ketones, alcohols, carboxylic acids). Components of the alcohol and the fatty acid fractions were derivatized with *bis*(trimethylsilyl)-fluoroacetamide and BF₃ in methanol, respectively.

The four fractions were examined with coupled gas chromatography – mass spectrometry (GC-MS) with a Thermo Scientific Trace GC Ultra coupled to a Thermo Scientific DSQ II mass spectrometer and by comparison with published mass spectra. Quantification was done with a Thermo Scientific Trace GC 1310 with a flame ionization detector. Both gas chromatographs were equipped with a 30 m TG-5MS silica capillary column with a diameter of 0.25 mm and a film thickness of 0.25 μm . The GC-temperature program was used as follows: 50 °C for 3 min, ramping from 50 to 230 °C at 25 °C per min, hold at 230 °C for 2 min, ramping from 230° to 325 °C at 6 °C per min, 25 min at 325 °C. All indigenous compounds were already cleared from the ketone and alcohol fractions due to thermal degradation. Thus, only the hydrocarbon and fatty acid fractions are discussed herein. Compound-specific carbon isotopes were measured on a gas chromatograph (Agilent 6890) coupled to a Thermo Finnigan Combustion III interface and a Thermo Finnigan Delta Plus isotope mass spectrometer (GC-IRMS). The GC column conditions were identical to those above, except for the temperature gradient: 50 °C for 3 min, ramping from 50 to 325 °C at 6 °C per min, hold for

20 min at 325 °C. All $\delta^{13}\text{C}$ values are reported in per mil relative to the VPDB standard and are corrected for the addition of carbon during derivatization procedures (cf. Birgel *et al.* 2014). Standard deviation of the measurements was less than 0.8 ‰ and accuracy was verified with a reference standard Mixture B (Arndt Schimmelmann, Indiana University, USA).

3. Results

3.a. Thin-section inventory

In the studied Bullman Creek limestone (Fig. 2a), echinoid fossils are enclosed by a matrix of pyritiferous micrite and minor microcrystalline aragonite, containing abundant detrital quartz (Fig. 2b). Banded and botryoidal fibrous cement consists of either calcite or aragonite, the latter representing the pristine mineralogy. Preservation of aragonite is evidenced by blunt crystal terminations (Fig. 2c), typical for the orthorhombic crystal habit of aragonite and the Feigl's stain. Fibrous cements originate on micrite (i.e. microcrystalline calcite), microcrystalline aragonite (Fig. 3a) and echinoid tests (Fig. 3b). Part of the fibrous aragonite cement is replaced by authigenic quartz (Fig. 3c), which is common, occurring also as large crystals within cavities or as microcrystals within the microcrystalline matrix. The latest paragenetic phase is equant calcite cement, filling the cavity centres and echinoid tests (Fig. 3b, d). Two types of equant calcite can be distinguished: an earlier, calcite cement and a later, ferroan calcite cement (Fig. 3d). Echinoid test fragments and spines are highly abundant (Fig. 3e). Apart from echinoids, the fossil inventory contains a few foraminifers, gastropods (Fig. 3f) and a single fragment of possibly crustacean origin.

3.b. Carbon and oxygen stable isotopes of carbonates

A total of 15 samples for stable isotope compositions was measured from the seven rock samples of the Bullman Creek echinoid deposit (Fig. 4). $\delta^{13}\text{C}$ values for micrite range from -16.6 ‰ to -12.7 ‰. Strong depletion of ^{13}C was noticed for fibrous cement, with low values from -23.5 ‰ to -21.1 ‰. Late diagenetic equant calcite cements yielded $\delta^{13}\text{C}$ values above 0 ‰ with a range from $+2.5$ ‰ to $+3.9$ ‰. The $\delta^{18}\text{O}$ values of micrite range from -8.6 ‰ to -2.9 ‰. Fibrous cements yielded values between -0.9 ‰ and $+1.9$ ‰. Analogously, $\delta^{18}\text{O}$ values of equant calcite cements vary little but are ^{18}O -depleted with values from -11.4 ‰ to -10.8 ‰.

3.c. Biomarker inventory

The overall biomarker inventory of the Bullman Creek echinoid deposit was analysed, but only the hydrocarbon (Fig. 5a) and fatty acid fractions (Fig. 5b) were found to contain indigenous compounds. The complete biomarker inventory is provided in the Supplementary Material (Tables S1 and S2). By far the most abundant compound within the hydrocarbon fraction is the regular isoprenoid phytane (2,6,10,14-tetramethylhexadecane), co-eluting with the irregular isoprenoid crocetane (2,6,11,15-tetramethylhexadecane). Further isoprenoids identified are PMI (2,6,10,15,19-pentamethylcosane), pristane (2,6,10,14-tetramethylpentadecane), biphytane (3,7,11,15,18,22,26,30-octamethyldotriacontane) as well as minor amounts of monocyclic biphytane and bicyclic biphytane. Among the *n*-alkanes, which range from 14 to 35 carbons, C_{16} and C_{17} are most abundant; chains longer than 25 carbons were only found in traces. Other than alkanes and

acyclic isoprenoids, various steroids are preserved, including 5 α -stigmastanes, 5 α -ergostanes, lanostane and 5 α -cholestane (20S). A second group of detected cyclic terpenoids are hopanes, including 17 α (H),21 β (H)- C_{30} -hopane, 17 α (H),21 β (H)- C_{31} -hopane (22S + R) and 17 α (H),21 β (H)- C_{35} -hopane. Other cyclic terpenoids detected are oleanane and gammacerane.

The fatty acid fraction is dominated by *n*-fatty acids ranging from C_9 to C_{32} and peaking at *n*- C_{16} . The latter compound depicts the largest peak of the fatty acid fraction. Short-chain terminally branched *iso*- and *anteiso*-fatty acids (C_9 – C_{19}) are common and peak at C_{15} . *Iso*-fatty acids are more abundant than their *anteiso*-counterparts. In addition, the sample yielded isoprenoid fatty acids ranging in chain length from C_{12} to C_{16} . The second most abundant compound of the fraction is 3,7,11,15-tetramethylhexadecanoic acid (phytanoic acid). Furthermore, minor 3,7,11,15,19-pentamethylcosanoic acid (PMI acid) was detected. Cyclic terpenoids were identified, including 17 α (H),21 β (H)- C_{32} -hopanoic (22R) acid, 17 β (H),21 α (H)- C_{32} -hopanoic (22R) acid and 17 β (H),21 β (H)- C_{32} -hopanoic (22R) acid. In addition, the sample contains a series of α,ω -diacids ranging from C_9 to C_{22} . These compounds have also been reported from a Cretaceous seep deposit of the Tarfaya Basin, Morocco (Smrzka *et al.* 2017), but their source is unknown.

3.d. Palaeontology

The fossil inventory consists almost exclusively of echinoid fossils, apparently of a single species of the order Spatangoida Agassiz, 1840. Unfortunately, a complete taxonomic description is not possible because the specimens can only be studied in cross-sections. The assignment to Spatangoida is based on the cross-section of the corona (Fig. 6a), which revealed the presence of aboral petal grooves (Fig. 6b), and the anterior displacement of the peristome (mouth; Fig. 6a). Both characters are indicative for irregular echinoids (Smith, 1984). The preservation of the echinoids is highly variable, including disarticulated ambulacral plates, which constitute the majority of echinoid remains, echinoid spines and a few intact tests. However, none of the tests have spines still attached to them. The shape of wedges and perforation of the cylinder of the echinoid spines suggests affiliation with Spatangoida rather than Holasteroida Durham & Melville, 1957 (Fig. 6c–e; Schlüter *et al.* 2015). A single specimen belongs to a regular echinoid as indicated by the cross-section of the corona and the large, once spine-bearing tubercles (Fig. 6f). While the echinoid tests do not display a preferred orientation and include overturned individuals as well as some in life position, the geopetal fillings within the tests show an approximately homologous orientation (Fig. 2a).

Other fossils seen in the Bullman Creek echinoid deposit include a single planktic foraminifer (a species of either *Globigerina* or *Globigerinoides*), two benthic foraminifers (a species of each *Bulimina* and *Nodosaria* or *Stilostomella*), two small, unidentified gastropods (Fig. 3f) and a possible crustacean fragment. Surprisingly, fossils of typical seep biota (e.g. siboglinid tube-worms, solemyid, bathymodiolin, thyasirid, lucinid and vesicomid bivalves) are absent from the Bullman Creek echinoid deposit. It should be stressed that all observations apply to the single block of limestone studied here; other limestone blocks from the same strata did not yield echinoids but instead contained typical seep-inhabiting bivalves, e.g. vesicomids, bathymodiolins, solemyids and lucinids (Kiel & Amano, 2013), thyasirids (Hryniewicz *et al.* 2017) and the gastropod *Provanna* (Squires, 1995).

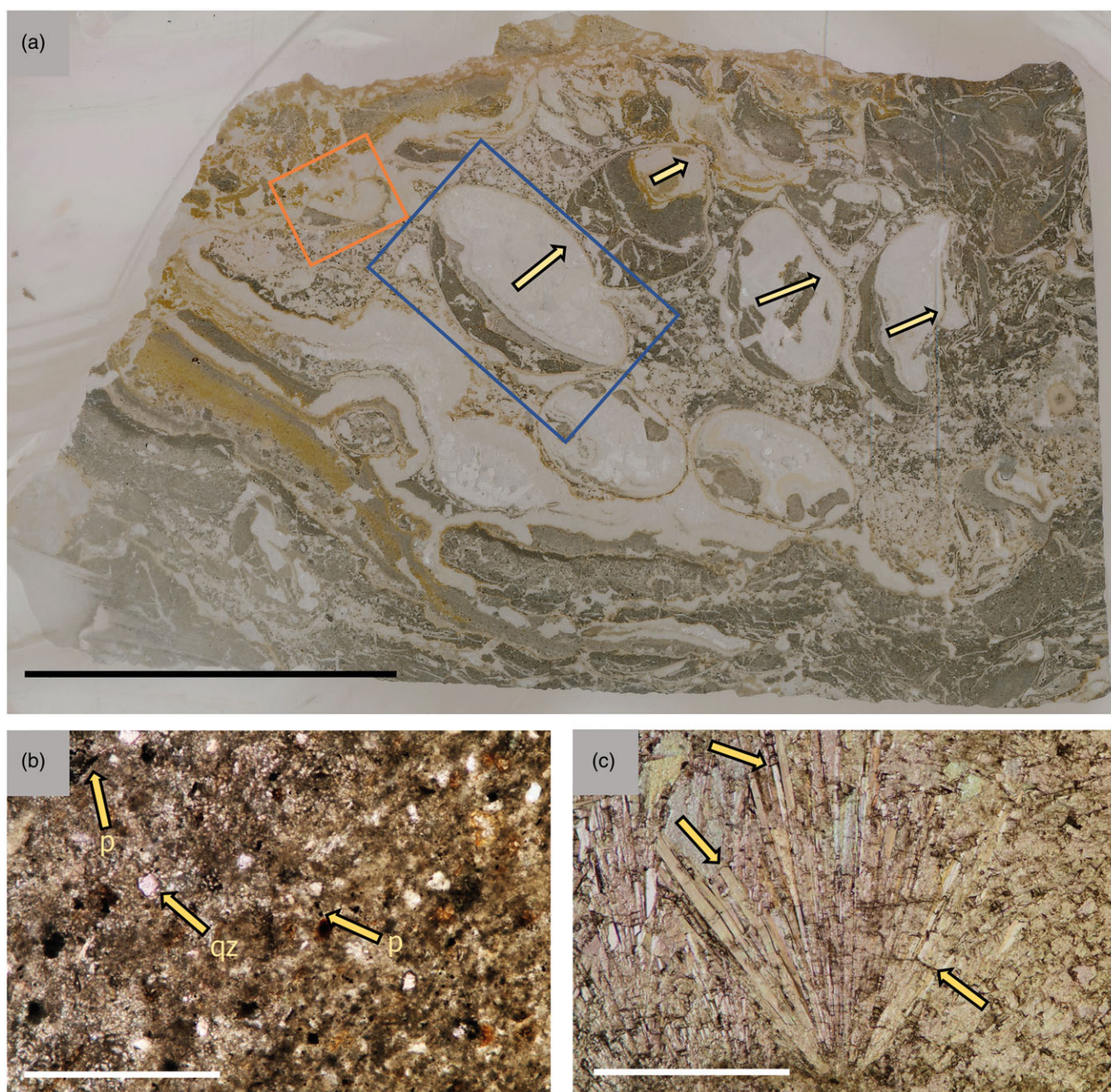


Fig. 2. (Colour online) Petrography of the Bullman Creek echinoid deposit. (a) Total view of thin-section. Arrows indicate original upward orientation based on geopetal fillings. Echinoid within blue frame enlarged in Figure 6a. Echinoid within orange frame enlarged in Figure 6f. (b) Matrix micrite with small quartz grains (light) and pyrite crystals (black). (c) Detail of a fibrous cement fan. Arrows show blunt crystal terminations indicating aragonite mineralogy. Scale bar of (a) equals 5 cm. Scales of (b) and (c) equal 500 μm . *p* – pyrite; *qz* – quartz.

4. Discussion

4.a. A hydrocarbon seep and its depositional environment

Petrography, stable carbon isotope compositions of authigenic carbonate minerals as well as biomarkers and their compound specific isotope compositions reveal that the echinoid-bearing Bullman Creek limestone is a methane-seep deposit. The limestone comprises a paragenetic sequence – pyritiferous microcrystalline matrix, fibrous banded and botryoidal cement, early diagenetic authigenic quartz, and late diagenetic equant calcite cement – typical of seep limestones (cf. Beauchamp & Savard 1992; Goedert *et al.* 2000; Peckmann *et al.* 2001; Campbell *et al.* 2002; Smrzka

et al. 2015; Zwicker *et al.* 2015). Authigenic carbonate minerals are depleted in ^{13}C , with $\delta^{13}\text{C}$ values as low as -23.5‰ (fibrous cement) and an average $\delta^{13}\text{C}$ value of -13.6‰ for micrite. Thus, both micrite and fibrous cements are significantly depleted in ^{13}C compared to marine dissolved inorganic carbon, agreeing with methane as a major but not exclusive carbon source (e.g. Peckmann & Thiel, 2004).

The biomarker inventory is dominated by compounds of an AOM consortium, confirmed by $\delta^{13}\text{C}$ values as low as -106‰ for the irregular archaeal isoprenoid hydrocarbon PMI. PMI is accompanied by the irregular C_{20} isoprenoid crocetane, which co-elutes with the regular C_{20} isoprenoid phytane; the latter

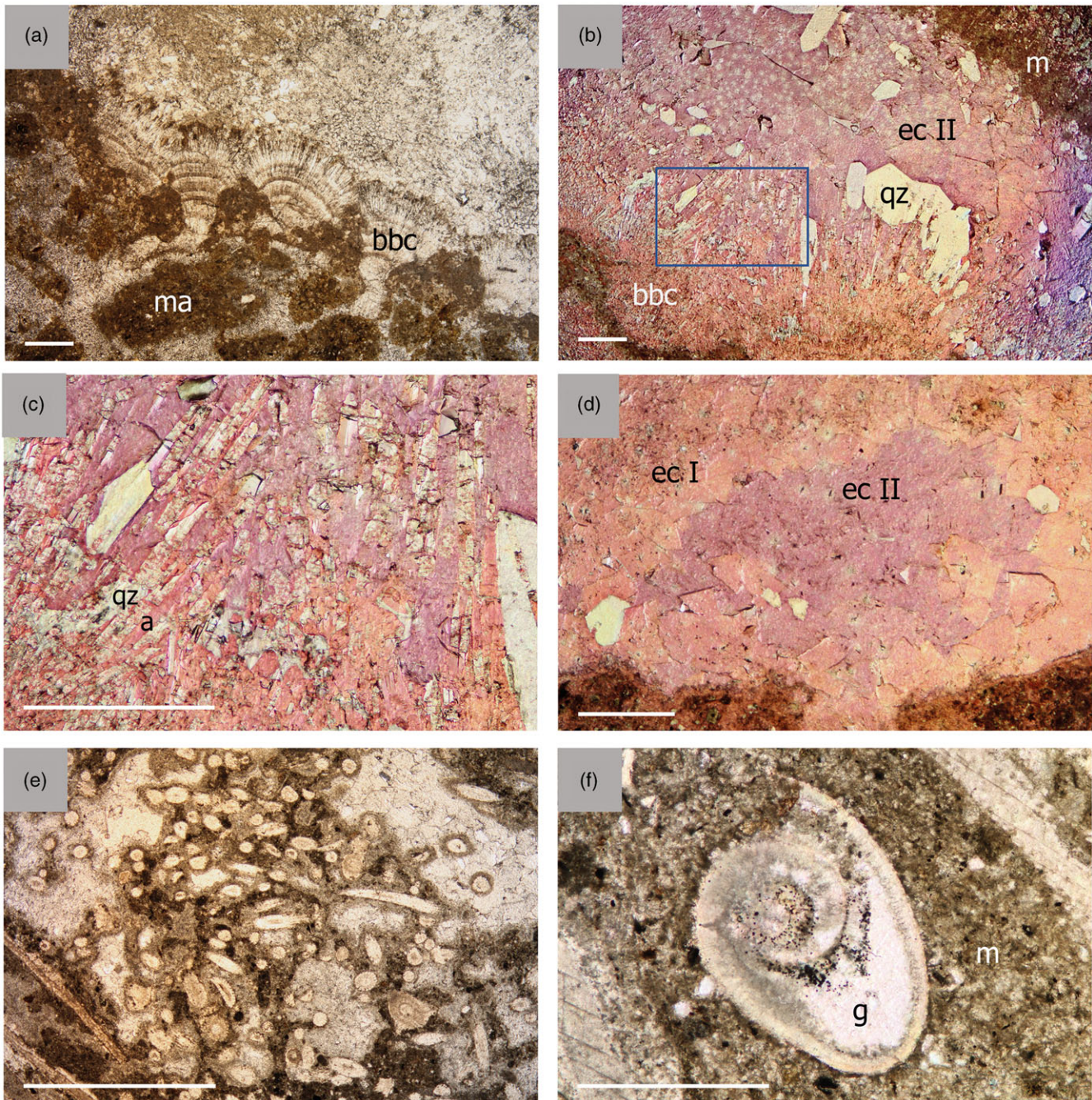


Fig. 3. (Colour online) Petrography of the Bullman Creek echinoid deposit. (a) Botryoidal fibrous cement postdating microcrystalline aragonite. (b) Stained thin-section showing a typical paragenetic sequence: fibrous aragonite cement originating from micrite, followed by equant calcite cement within an echinoid test. Staining reveals partial replacement of aragonite by quartz. The equant calcite cement in the centre of the cavity is enriched in iron. Area within blue frame enlarged in (c). (c) Detail of fibrous cement. Quartz (light crystals) replaces aragonite (orange-pinkish crystals at the lower margin). (d) Cavity filled with an equant calcite cement, followed by a ferroan equant calcite cement, stained thin-section. (e) Abundant echinoid spines and plate fragments within matrix micrite and aragonitic cement. (f) Unidentified gastropod, one of the rare non-echinoid fossils, enclosed by micrite. All photographs were taken under plane-polarized light. Scale bars equal 500 μm . *a* - aragonite; *bbc* - banded and botryoidal fibrous cement; *ec I* - equant calcite cement; *ec II* - ferroan equant calcite cement; *es* - echinoid spine; *g* - gastropod; *m* - micrite; *ma* - microcrystalline aragonite; *qz* - quartz.

represents a degradation product of archaeal diether lipids (combined peak $\delta^{13}\text{C}$: -103 ‰). The archaeal molecular fossils are accompanied by terminally branched fatty acids, namely *iso*- and *anteiso*- C_{15} fatty acids with higher $\delta^{13}\text{C}$ values (-72 ‰ and -79 ‰, respectively) than the ANME lipids, indicating contributions from sulphate-reducing bacteria involved in or benefiting from AOM.

Currently three groups of archaea (ANME-1, -2, -3) are known to be able to perform AOM in association with sulphate-reducing bacteria of either the DSS (*Desulfosarcina/Desulfococcus*) or the DBB (*Desulfobulbus*) clade. Previous studies noticed a correlation between the different types of AOM consortia and the intensity of seepage, concluding that ANME-1 and ANME-2 can be distinguished by their biomarker patterns (Blumenberg *et al.* 2004;

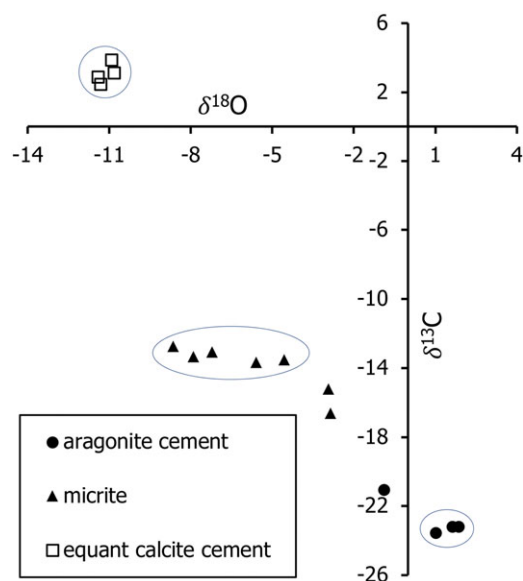


Fig. 4. Plot of stable isotope data of the Bullman Creek echinoid deposit; values are in per mil versus VPDB. Ovals indicate distinct isotope ranges of each phase. Data points outside ovals represent values that were possibly contaminated by another phase during micro drilling.

Niemann & Elvert, 2008). The biomarker inventory of the Bullman Creek echinoid deposit agrees with the dominance of ANME-2/DSS based on the abundant presence of crocetane (45 % of all hydrocarbons in combination with phytane); ANME-1 and ANME-3 only produce minor crocetane (cf. Niemann & Elvert, 2008). Further evidence for the dominance of ANME-2 consortia is provided by the lipids of their syntrophic partners and the *ai-C_{15:0}/i-C_{15:0}* ratio of 0.79 typical of sulphate-reducing bacteria associated with ANME-2 archaea (see Table 1 for compound contents; cf. Niemann & Elvert, 2008; Yao *et al.* 2021 and references therein). Finally, ANME-2 dominance at the Bullman Creek echinoid seep agrees with the abundance of fibrous cements (cf. Peckmann *et al.* 2009). ANME-1 were also subordinately present because minor (c. 3 % of all hydrocarbons) acyclic, monocyclic, and bicyclic biphytanes, degradation products of glycerol dibiphytanyl glycerol tetraethers, were detected (cf. Blumenberg *et al.* 2004; Niemann & Elvert, 2008; Peckmann *et al.* 2009). Overall, the combined petrographical and geochemical evidence suggests that the seepage from which the Bullman Creek echinoid limestone resulted was intense, favouring the establishment of chemosynthesis-based microbial communities on the Oligocene seafloor.

4.b. Palaeoecology and taphonomy

Echinoid remains are highly abundant in the studied Bullman Creek limestone, but intact tests are arranged randomly and most of them are not in life-orientation. This suggests that some transport was involved in the deposition of the echinoids. However, the variable degree of preservation of the echinoids does not agree with long-distance transport, transport by strong bottom currents, or mass mortality. Greenstein (1991) analysed the influence of tumbling on the preservation of echinoid tests and found that little mechanical stress is required to remove all spines from the tests or even destroy the tests. It needs to be stressed that Greenstein's study did not deal with irregular echinoids, and it concluded that the amount of disarticulation varies among different echinoids. However, compared to regular echinoids, coronal plates

of irregular echinoids are extremely thin (Fig. 6a, b; Kier, 1977) and lack interlocking structures within the coronal plates, being connected only by collagen fibres. Removal of this collagen results in rapid disarticulation of the test (Smith, 1984), especially if exposed at the seafloor at time of death (Kier, 1977). Bearing this in mind, major transport is unlikely to have been involved in the deposition of the Bullman Creek echinoids. Further evidence for this hypothesis comes from the homologous orientation of geopetal fills. Geopetals are a rather unusual feature in echinoids. This is due to large openings of the peristome and the periproct through which sediment enters the test after decay of the membranes that cover these openings in life. After death of the echinoid, these membranes disarticulate within one or two weeks (Smith, 1984). The presence of geopetals within Bullman Creek echinoid tests indicates that they were covered with sediment before these membranes decayed and sediment could fill up the whole cavity; the small amount of sediment observed in irregular echinoids with geopetal structures derives from the sediment present in the gut of the animals, many of which are deposit feeders.

Because fluid flow at seeps can vary significantly at short time-scales, fluid flow increase at the Bullman Creek echinoid seep might have led to lethal concentrations of hydrogen sulphide. As a result, most of the echinoids may have died due to their inability to escape in time from the site, as demonstrated in experiments by Riedel *et al.* (2008). Furthermore, brecciation of carbonate crusts is a common feature of seep deposits, indicating localized excess pore pressure caused by the accumulation of methane below the crusts (e.g. Beauchamp & Savard, 1992; Peckmann & Thiel, 2004). Such excess in gas pressure possibly led to brecciation of carbonates and the disruption of the upper sediment layers at the location of the Bullman Creek deposit (e.g. Hovland *et al.* 1987). Consequently, sediments, carbonates and living, dead and decaying echinoids were relocated over a short distance, partially disintegrated, and covered by sediment. Interestingly, Beauchamp & Savard (1992), Peckmann *et al.* (1999) and Birgel *et al.* (2006a) suggested *in situ* brecciation as a mechanism of temporary oxygenation at seeps. The biomarker inventory of the Bullman Creek echinoid deposit includes gammacerane and lanostane, both biomarkers of aerobic methanotrophic bacteria at seeps (Birgel & Peckmann, 2008; Cordova-Gonzalez *et al.* 2020). Thus, there is evidence for episodically or locally oxic conditions within the sediment at the Bullman Creek echinoid seep site. This hypothesized sequence of events is summarized in Figure 7, explaining the mass occurrence and deposition of echinoids within the Bullman Creek echinoid deposit.

4.c. Echinoids at hydrocarbon seeps

Notwithstanding more than 30 years of research on fossil seep deposits in western Washington State, the new limestone described herein is unique for its fossil inventory, which consists almost entirely of echinoid remains. Spatangoid fragments were reported from another Oligocene seep deposit in Washington (SR4 of Peckmann *et al.* 2002) but these were only minor components of the preserved fauna. The association of echinoderms (crinoids, echinoids, asteroids, ophiuroids) with seep carbonate in the Keasey Formation in northwest Oregon was documented by Burns *et al.* (2005), but whether these animals were using carbonate as a hard-ground or were part of a seep community has not been firmly established. Echinoids have only infrequently been reported from modern seeps and only few species occur in greater abundance in these habitats, with the intensity of sulphide flux as the apparently

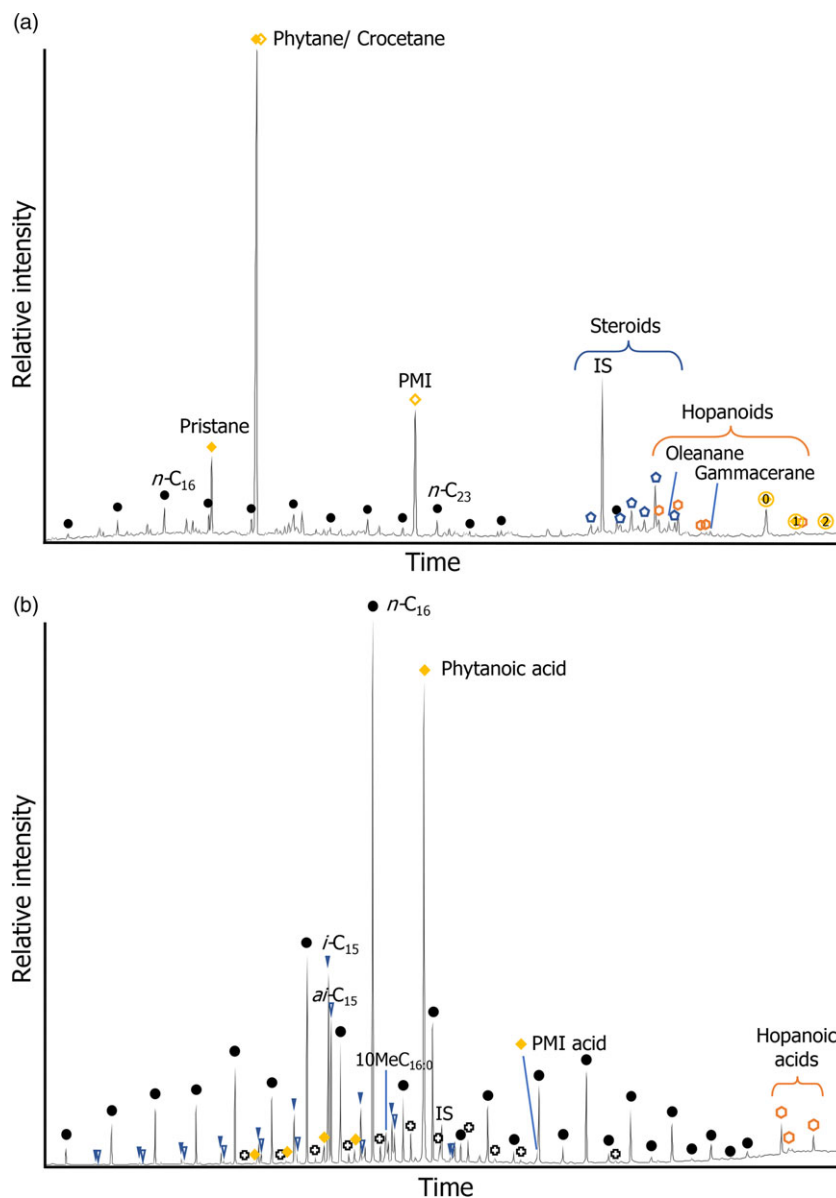


Fig. 5. (Colour online) Biomarker inventory of the Bullman Creek echinoid deposit. (a) Total ion-chromatogram of the hydrocarbon fraction. Black circles: *n*-alkanes (C_{14-23} , C_{29}); yellow diamonds: regular (filled) and irregular (open) isoprenoids; circled yellow diamonds: biphytanes with number of rings; blue pentagons: steroids; orange hexagons: hopanoids; IS = internal standard. (b) Total ion-chromatogram of the fatty acid fraction. Black circles: *n*-fatty acids; blue triangles: *iso*- (filled) and *anteiso*- (open) fatty acids; orange hexagons: hopanoic acids; yellow diamonds: isoprenoic acids; crosses: α,ω -diacids; IS = internal standard.

limiting condition (Sahling *et al.* 2002). Among extant echinoids, the genera *Gracilechinus* and *Echinus* show a greater tolerance towards sulphide; *Gracilechinus alexandri* Danielssen & Koren, 1883 is widely distributed in the North Atlantic Ocean and has been reported from methane seeps from the Gulf of Mexico (Pawson *et al.* 2015) and the Lucky Strike hydrothermal vent field (Desbruyères *et al.* 2001). *Gracilechinus multidentatus* Clark, 1925 was found around the Tui seep site at Hikurangi Margin, New Zealand (Bowden *et al.* 2013). *Echinus* sp. was reported from the Napoli and Kazan mud volcanoes in the Mediterranean Sea (Olu *et al.* 2004) and from vents at the southern East Pacific Rise (Desbruyères *et al.* 2006). Isotope analysis of tissue of the Mediterranean seep *Echinus* sp. yielded $\delta^{13}C$ values from -42.3 ‰ to -35.7 ‰, revealing incorporation of AOM-derived carbon likely derived by feeding on bacterial mats (Olu *et al.* 2004). Furthermore, Olu *et al.* (2004) emphasized that *Echinus* sp. had a patchy distribution in the seep areas and was absent from the inactive periphery of the seep sites. Although this species also occurs in the surroundings, it is attracted by the increased food

supply at seeps, apparently relying to a large extent on AOM-derived biomass. Likewise, Rybakova *et al.* (2022) found the echinoid *Brisaster latifrons* in great abundance on bacterial mats at seeps in the Bering Sea. The carbon isotope signature of its soft tissue indicated a notable, though minor, contribution of methane-derived carbon to its diet (Rybakova *et al.* 2022). A potential fossil example of such echinoids that took advantage of the abundant biomass at methane seeps is the regular echinoid *Salenia* sp. from the Upper Cretaceous Tepee Buttes in South Dakota, USA (Kato *et al.* 2017).

Of all modern echinoids, the most probable candidate to be endemic to seeps is the irregular echinoid *Sarsiaster griegii* Mortensen, 1950, from the order Spatangoida. Originally described from a single specimen from the North Atlantic Ocean at a depth of 3120 m (Mortensen, 1950), this species was reported from (1) the Venezuelan Basin at 3450 m (Briggs *et al.* 1996), (2) Blake Ridge (NW Atlantic Ocean) hydrocarbon seeps below 2000 m water depth at the outer margin of vesicomid beds, but not in the periphery of the site (Van Dover *et al.* 2003), (3) sediments rich

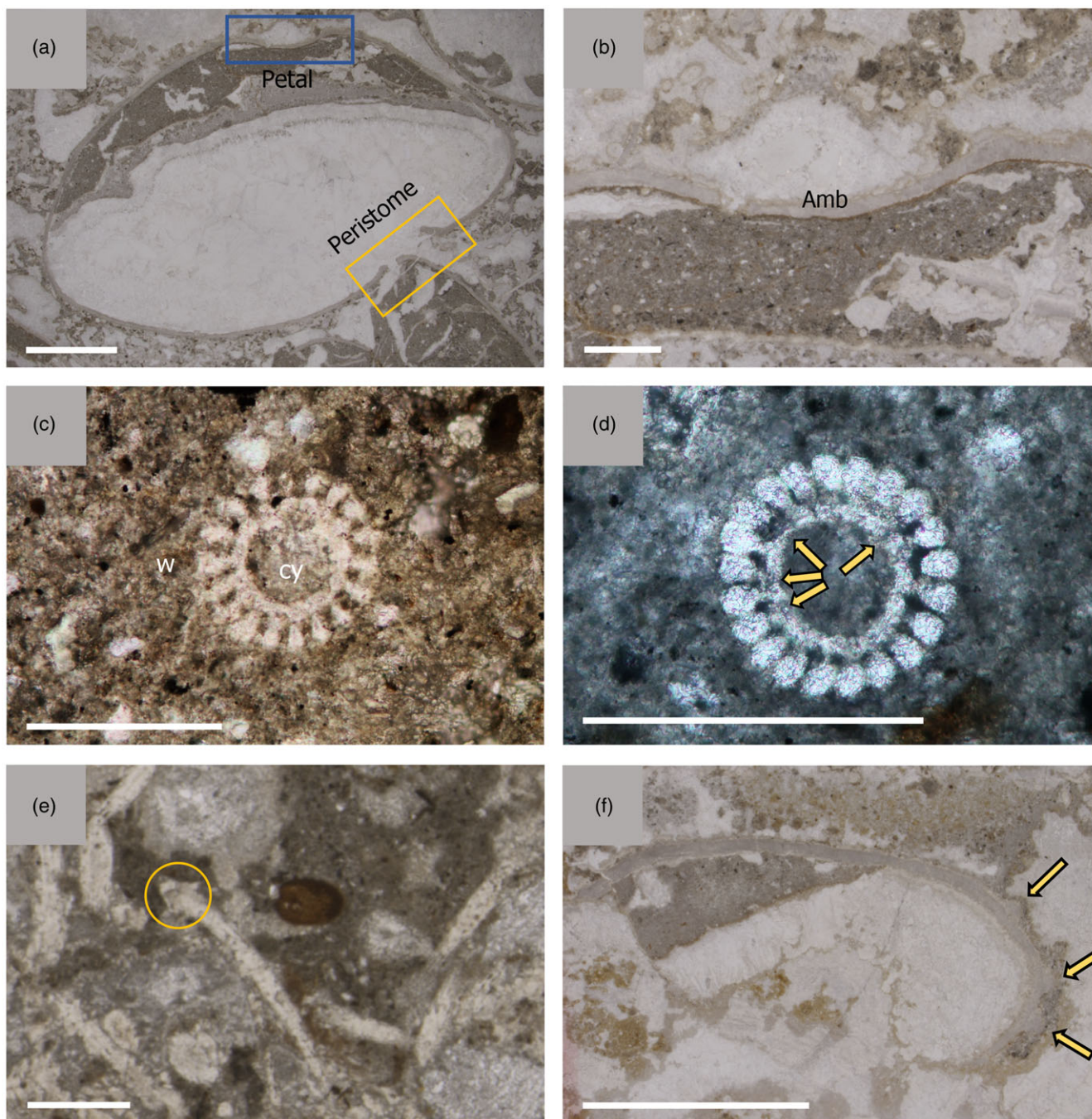


Fig. 6. (Colour online) Echinoids in thin-sections of the Bullman Creek limestone. (a) Cross-section of spatangoid echinoid fossil (note that the specimen is not in life position as indicated by the geopetal structure with sediment accumulated in the dorsal third of the body cavity). Yellow frame shows position of the peristome (mouth). Blue frame enlarged in (b). (b) Cross-section through a petal. (c, d) Cross-sections of echinoid spines. Shape of wedges resembles modern spatangoids (c). The arrows in (d) highlight the irregular perforations of the cylinder. (e) Longitudinal section of an echinoid spine. Yellow circle shows the broad base; notice the bend typical of spatangoid echinoids. (f) Cross-section of a regular echinoid test; arrows indicate the tubercles to which the spines are attached in life. All photographs were taken under plane-polarized light. Scale bars equal 0.5 cm (a, f), 1000 μ m (b) and 250 μ m (c-e); *Amb* – ambulacrum; *cy* – cylinder; *w* – wedge.

in hydrogen sulphide at a brine pool in Alaminos Canyon (site AC-601) in the Gulf of Mexico at 2300 m water depth (Cordes *et al.* 2010) and (4) again from Alaminos Canyon (sites AC-340, AC-818) at 2100 to 2800 m water depth (SA Lessard-Pilon, unpub. PhD thesis, Pennsylvania State Univ., 2010; Lessard-Pilon *et al.* 2010). Lessard-Pilon *et al.* (2010) described aggregations of *S. griegii* covering areas as large as 10 000 m², occurring in high abundances along mats of sulphide-oxidizing bacteria. Siboglinid

tubeworms and bathymodiolin mussels were present but much less abundant compared to other seep sites of the Gulf of Mexico. Lessard-Pilon *et al.* (2010) noticed high sulphide concentration at one of the examined sites and stressed that AOM rates were among the highest measured at seeps in the Gulf of Mexico. Echinoids were found to be epifaunal and did not change their position during a three-day observation. Apparently, the abundance of bacteria and thus increased food availability makes

Table 1. Biomarker inventory of the Bullman Creek echinoid seep deposit

Compound	$\delta^{13}\text{C}$ (‰)	Putative source	Precursor lipid
Phytanoic acid	-97	ANME	Archaeol
Phytane + crocetane	-103	ANME	Archaeol derivatives/ unsaturated crocetenes
PMI	-106	ANME	Unsaturated PMIs
Pristane	-86	ANME, algae	Archaeol, α -tocopherol, chlorophyll
Acyclic biphytane	-97	ANME	GDGT-0
Monocyclic biphytane	n.m.	ANME	GDGT-1, -2
Bicyclic biphytane	n.m.	ANME	GDGT-3
<i>Iso</i> -C ₁₅ acid	-72	SRB	
<i>Anteiso</i> -C ₁₅ acid	-79	SRB	
<i>Iso</i> -C ₁₆ acid	-68	SRB	
Lanostane	n.m.	MOB	Lanosterol, 4-methyl sterols
17 α (H),21 β (H)-C ₃₀ - hopane	-60	MOB?	BHPs, diploptene
17 α (H),21 β (H)-C ₃₂ - hopanoic (22 <i>R</i>) acid	-62	MOB?	BHPs
Gammacerane	n.m.	MOB, ciliates	Tetrahymanol

Note: ANME – anaerobic methane-oxidizing archaea; BHPs – bacteriohopanepolyols; GDGT – glycerol dibiphytanyl glycerol tetraether; MOB – aerobic methane-oxidizing bacteria; PMI – 2,6,10,15,19-pentamethylcosane; SRB – sulphate-reducing bacteria; n.m. – not measured.

movement or burrowing unnecessary (Lessard-Pilon *et al.* 2010). Analysis of carbon stable isotope compositions of the tissue of *S. griegii* yielded $\delta^{13}\text{C}$ values between -41.0 ‰ and -32.9 ‰, indicating its participation in the local chemosynthesis-based food web. However, no morphological evidence for endosymbiosis was found after dissection of specimens (SA Lessard-Pilon, unpub. PhD thesis, Pennsylvania State Univ., 2010; Lessard-Pilon *et al.* 2010). *Sarsiaster griegii* can obviously tolerate high concentrations of hydrogen sulphide, and its abundance and distribution at multiple seep sites and sites typified by high levels of hydrogen sulphide agrees with a seep-related or even seep-restricted lifestyle. There are some remarkable similarities between the occurrence of the Bullman Creek echinoids and the Recent occurrences of *Sarsiaster griegii*, including high abundance of specimens, subordinate presence or even absence of typical seep fauna such as mussels, clams and tubeworms, and the fact that both species belong to the order Spatangoida. In addition, all the documented seep sites with *S. griegii* share a similar geochemical environment of high fluid flow, high rates of AOM and an ANME-2/DSS dominance. Therefore, it seems likely that the Bullman Creek echinoid deposit preserves an ancient analogue to the modern ecosystem dominated by *S. griegii* at Alaminos Canyon.

An interesting site of fossil seep-related echinoids is found in the Upper Jurassic Terres-Noires Formation at Beauvoisin in southern France, where numerous seep carbonate blocks are exposed (Gaillard *et al.* 1992, 2011). Within one of the blocks, the irregular echinoid *Tithonia oxfordiana* dominates the benthic faunal assemblage, comprising 63 % of all invertebrate fossil

specimens, whereas typical seep-dwelling lucinid bivalves represent only 36 %. Intriguingly, *T. oxfordiana* was found solely on top of the seep deposit. Gaillard *et al.* (2011) interpreted the colonization by *T. oxfordiana* as ephemeral and suggested a mass dying of the population in the final phase of seepage, triggered by the release of some toxic substance. The latter agrees with the scenario we propose for the ecology and deposition of the Bullman Creek echinoids (Fig. 7), in accord with the observation Gaillard *et al.* (2011) made for *T. oxfordiana*, which were found to be rarely, if ever, transported and thus were probably found in their original habitat. Notwithstanding the similarities between the Bullman Creek echinoid deposit and the *Tithonia* deposit, two uncertainties remain. (1) The biomarker inventory of some of the Beauvoisin seep deposits, all of similar age and composition to the deposit with *T. oxfordiana*, was studied by Peckmann *et al.* (1999). However, the *n*-alkane pattern revealed that the *Tithonia* deposit was affected by thermal maturation; therefore, the composition of the Oxfordian AOM community and, thus, the geochemical environment remained largely unconstrained. (2) Taxonomic position of the echinoid remains from the Bullman Creek echinoid deposit is still poorly constrained. Available data suggest that adaptation to seep environments developed in at least two different irregular echinoid lineages (Spatangoida: *Sarsiaster* and stem-group Atelostomata: *Tithonia*, cf. Barras, 2007; Kroh *et al.* 2014). The taxonomic position of the Bullman Creek echinoids is therefore of vital interest as it may shed further light on the adaptation of echinoids to chemosynthesis-based environments.

5. Conclusions

The Bullman Creek echinoid seep deposit represents an ancient methane-seep deposit. Evidence for this interpretation stems from compound-specific carbon stable isotope compositions of molecular fossils of methanotrophic archaea as low as -106 ‰ and the paragenetic sequence of the limestone, including pyritiferous matrix micrite, fibrous botryoidal and banded cement, authigenic quartz and late diagenetic equant calcite cements, resembling other seep deposits. The AOM community was dominated by an ANME-2/DSS consortium typical of higher fluid flow sites as evidenced by the abundant presence of crocetane with possibly minor contributions of an ANME-1/DSS consortium; the abundance of fibrous cements and the scarcity of biphytanes support this interpretation. In addition to molecular fossils of the AOM community, the biomarker inventory includes gammacerane and lanostane, indicating the presence of aerobic methanotrophic bacteria at the Oligocene seep. The fossil inventory of the Bullman Creek echinoid deposit did not yield a single specimen of typical seep biota (chemosymbiotic bivalves, bacterial mat-grazing gastropods, siboglinid tubeworms). Instead, it consists almost entirely of echinoid remains, belonging to a species of an unidentified spatangoid. A single specimen of a regular echinoid was found as well. The high abundance of spatangoid specimens resembles the occurrences of the fossil *T. oxfordiana* and the modern spatangoid *Sarsiaster griegii*, which are known from hydrocarbon seeps, sometimes dominating the faunal composition in biomass and abundance. *Sarsiaster griegii* favours seeps with a strong fluid-flow where it feasts on extensive bacterial mats. Evidence that the Bullman Creek echinoids were part of the seep community is given by the variable preservation of the fossils, which is explained by the parautochthonous nature of the echinoid assemblage. This is the first report of spatangoids dominating the macrofaunal assemblage of a fossil hydrocarbon-seep deposit. Thus, this work extends the

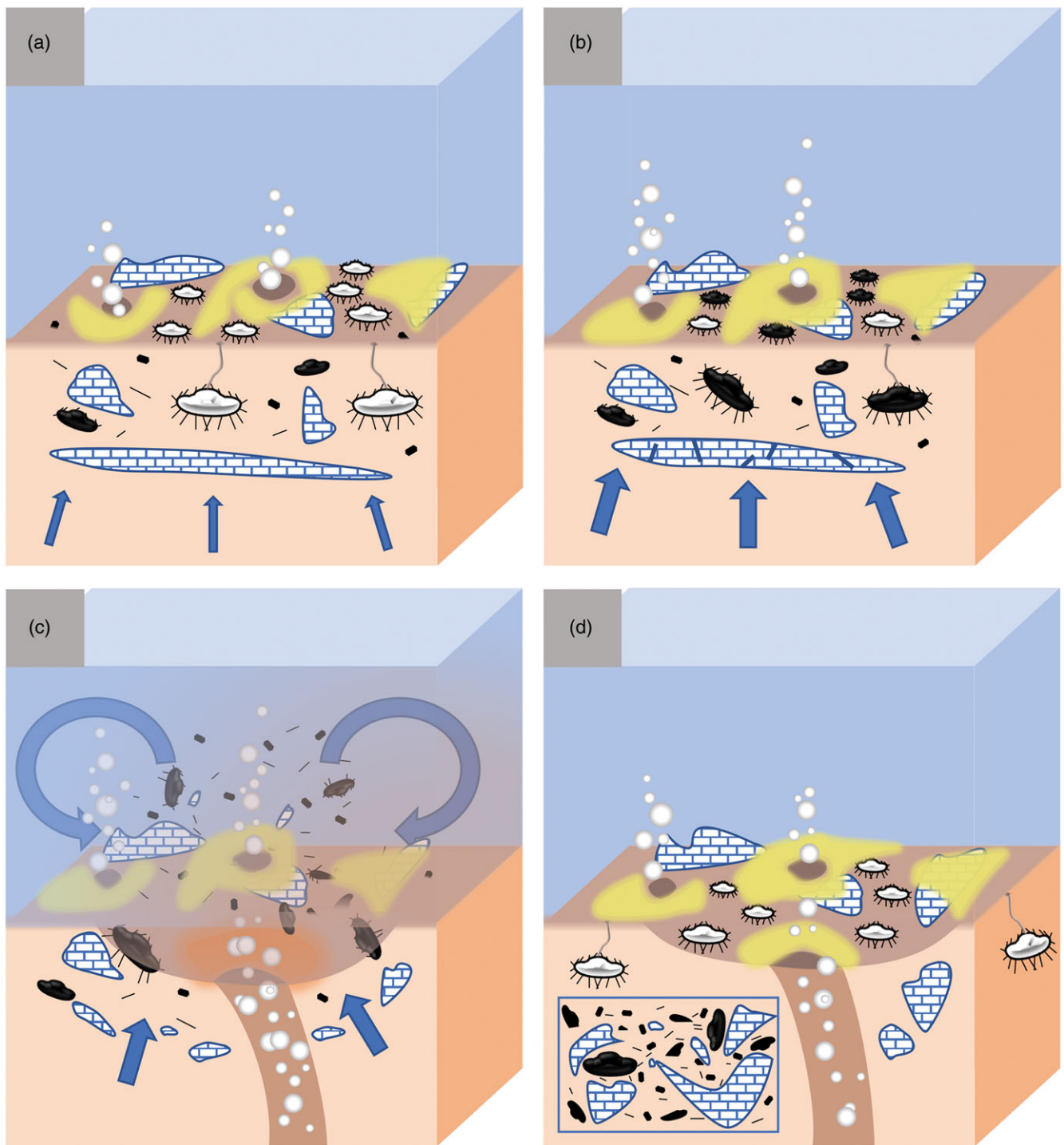


Fig. 7. (Colour online) Deposition model for echinoids at the Bullman Creek echinoid seep. (a) Active hydrocarbon seep with strong fluid-flow, dominated by irregular echinoids and microbial mats (yellow). Notice that some echinoids advance into anoxic sediment and occur next to authigenic carbonates (blue-white bricks) and bacterial mats on top of it. Dead echinoids in various states of decay occur as well. Black fragments represent echinoid plates (hexagons) and echinoid spines (bars). Below the seep carbonates, methane accumulates, increasing the pore pressure (blue arrows). (b) Increase of fluid-flow leads to death of most echinoids (black) due to enhanced hydrogen sulphide flux and possible anoxia close to or at the seafloor; microbial mats grow, and carbonates keep on forming. Further increase of pore pressure (blue arrows). (c) Excess pore pressure leads to *in situ* brecciation. Methane and sediment reach the seafloor, mixing with ocean water provides molecular oxygen. Temporary localized dominance of aerobic methane-oxidizing bacteria (orange). Outburst of methane leads to partial disarticulation of echinoid carcasses and slight relocation of echinoids. Echinoid remains get covered with sediment. (d) Like (a), below the upper sediments, remains of echinoids are preserved within seep limestones. Blue frame represents the Bullman Creek echinoid seep deposit.

knowledge about echinoids at high-flux seeps and elucidates that spatangoid adaptation to chemosynthesis-based ecosystems dates back at least to the earliest Oligocene.

Supplementary material. To view supplementary material for this article, please visit <https://doi.org/10.1017/S0016756823000067>.

Acknowledgements. We thank Birgit Leipner-Mata (Erlangen) for the preparation of thin-sections, Gerhard Schmiedl (Hamburg) for help with the identification of foraminifera and Sabine Beckmann (Hamburg) for her valuable support in the biomarker preparation. Insightful comments by Krzysztof Hryniewicz (Warsaw) and an anonymous reviewer substantially improved the manuscript.

Declaration of interest. There is no conflict of interest to report.

References

- Amano K and Kiel S (2007) Fossil vesicomid bivalves from the North Pacific Region. *Veliger* **49**, 270–93.
- Barras CG (2007) Phylogeny of the Jurassic to Early Cretaceous “disasteroid” echinoids (Echinoidea; Echinodermata) and the origins of spatangoids and holasteroids. *Journal of Systematic Palaeontology* **5**, 134–61.
- Beauchamp B and Savard M (1992) Cretaceous chemosynthetic carbonate mounds in the Canadian Arctic. *Palaios* **7**, 434–50.
- Birgel D, Guido A, Liu X, Hinrichs K-U, Gier S and Peckmann J (2014) Hypersaline conditions during deposition of the Calcare di Base revealed from archaeal di- and tetraether inventories. *Organic Geochemistry* **77**, 11–21.
- Birgel D and Peckmann J (2008) Aerobic methanotrophy at ancient marine methane seeps: a synthesis. *Organic Geochemistry* **39**, 1659–67.
- Birgel D, Peckmann J, Klautzsch S, Thiel V and Reitner J (2006a) Anaerobic and aerobic oxidation of methane at Late Cretaceous seeps in the Western Interior Seaway, USA. *Geomicrobiology Journal* **23**, 565–77.
- Birgel D, Thiel V, Hinrichs K-U, Elvert M, Campbell KA, Reitner J, Farmer JD and Peckmann J (2006b) Lipid biomarker patterns of methane-seep microbialites from the Mesozoic convergent margin of California. *Organic Geochemistry* **37**, 1289–1302.
- Blumenberg M, Seifert R, Reitner J, Pape T and Michaelis W (2004) Membrane lipid patterns typify distinct anaerobic methanotrophic consortia. *PNAS* **101**, 11111–16.
- Boetius A, Ravensschlag K, Schubert CJ, Rickert D, Widdel F, Gieseke A, Amann R, Jørgensen BB, Witte U and Pfannkuche O (2000) A marine microbial consortium apparently mediating anaerobic oxidation of methane. *Nature* **407**, 623–6.
- Bowden DA, Rowden AA, Thurber AR, Baco AR, Levin LA and Smith CR (2013) Cold seep epifaunal communities on the Hikurangi Margin, New Zealand: composition, succession, and vulnerability to human activities. *PLOS ONE* **8**, e76869.
- Brandon M, Roden-Tice M and Garver J (1998). Late Cenozoic exhumation of the Cascadia accretionary wedge in the Olympic Mountains, northwest Washington State. *Geological Society of America Bulletin* **110**, 985–1009.
- Brandon MT and Vance JA (1992) Tectonic evolution of the Cenozoic Olympic subduction complex, Washington State, as deduced from fission track ages for detrital zircons. *American Journal of Science* **292**, 565–636.
- Brezina J, Larson NL and Landman NH (2022) Echinoderms at ancient hydrocarbon seeps and cognate communities. In *Ancient Hydrocarbon Seeps* (eds A Kaim, JK Cochran and NH Landman), pp. 407–18. *Topics in Geobiology* **50**. Cham: Springer.
- Briggs KB, Richardson MD and Young DK (1996) The classification and structure of megafaunal assemblages in the Venezuela Basin, Caribbean Sea. *Journal of Marine Research* **54**, 705–30.
- Burns C, Campbell KA and Mooi R (2005) Exceptional crinoid occurrences and associated carbonates of the Keasey Formation (early Oligocene) at Mist, Oregon, USA. *Palaeogeography, Palaeoclimatology, Palaeoecology* **227**, 210–31.
- Burns C and Mooi R (2003) An overview of Eocene-Oligocene echinoderm faunas of the Pacific Northwest. In *From Greenhouse to Icehouse* (eds DR Prothero, LC Ivany and EA Nesbitt), pp. 88–106. New York: Columbia University Press.
- Campbell KA (1992) Recognition of a Mio-Pliocene cold seep setting from the Northeast Pacific Convergent Margin, Washington, U.S.A. *Palaios* **7**, 422–33.
- Campbell KA (2006) Hydrocarbon seep and hydrothermal vent paleoenvironments and paleontology: past developments and future research directions. *Palaeogeography, Palaeoclimatology, Palaeoecology* **232**, 362–407.
- Campbell KA, Farmer JD and des Marais D (2002) Ancient hydrocarbon seeps from the Mesozoic convergent margin of California: carbonate geochemistry, fluids and paleoenvironments. *Geofluids* **2**, 63–94.
- Carney RS (2010) Stable isotope trophic patterns in echinoderm megafauna in close proximity to and remote from Gulf of Mexico lower slope hydrocarbon seeps. *Deep-Sea Research Part II: Topical Studies in Oceanography* **57**, 1965–71.
- Cochran KJ, Landman NH, Brezina J, Naujokaityte J, Rashkova A, Garb MP and Larson NL (2022) Geochemistry of cold hydrocarbon seeps: an overview. In *Ancient Hydrocarbon Seeps* (eds A Kaim, JK Cochran and NH Landman), pp. 3–45. *Topics in Geobiology* **53**. Cham: Springer.
- Cordes EE, Hourdez S and Roberts HH (2010) Unusual habitats and organisms associated with the cold seeps of the Gulf of Mexico. In *The Vent and Seep Biota* (ed. S Kiel), pp. 315–31. *Topics in Geobiology* **33**. Dordrecht: Springer Science+Business Media.
- Cordova-Gonzalez A, Birgel D, Kappler A and Peckmann J (2020) Carbon stable isotope patterns of cyclic terpenoids: a comparison of cultured alkaliphilic aerobic methanotrophic bacteria and methane-seep environments. *Organic Geochemistry* **139**, 1–14.
- Desbruyères D, Biscoito M, Caprais J-C, Colaço A, Comtet T, Crassous P, Fouquet Y, Khripounoff A, Le Bris N, Olu K, Riso R, Sarradin P-M, Segonzac M and Vangriesheim A (2001) Variations in deep-sea hydrothermal vent communities on the Mid-Atlantic Ridge near the Azores plateau. *Deep-Sea Research I* **48**, 1325–46.
- Desbruyères D, Segonzac M and Bright M (2006) *Handbook of Deep-Sea Hydrothermal Vent Fauna*, second completely revised version. *Denisia* **18**. 544 pp. Linz: Biologiezentrum der Oberösterreichischen Landesmuseen.
- Dickson JAD (1966) Carbonate identification and genesis as revealed by staining. *Journal of Sedimentary Petrology* **36**, 491–505.
- Dubilier N, Bergin C and Lott C (2008) Symbiotic diversity in marine animals: the art of harnessing chemosynthesis. *Nature Reviews Microbiology* **6**, 725–40.
- Feigl F (1958) *Spot Test in Inorganic Analysis, fifth enlarged and revised English edn*. Amsterdam: Elsevier, 600 pp.
- Gaillard C, Néraudeau D and Thierry J (2011) *Tithonia oxfordiana*, a new irregular echinoid associated with Jurassic seep deposits in south-east France. *Palaeontology* **54**, 735–52.
- Gaillard C, Rio M, Rolin Y and Roux M (1992) Fossil chemosynthetic communities related to vents or seeps in sedimentary basins: the pseudobioherms of southeastern France compared to other world examples. *Palaios* **7**, 451–65.
- Goedert JL and Campbell KA (1995) An early Oligocene chemosynthetic community from the Makah Formation, northwestern Olympic Peninsula, Washington. *Veliger* **38**, 22–9.
- Goedert JL and Peckmann J (2005) Corals from deep-water methane-seep deposits in Paleogene strata of western Oregon and Washington, U.S.A. In *Cold-Water Corals and Ecosystems* (eds A Freiwald and JM Roberts), pp. 27–40. Berlin and Heidelberg: Springer-Verlag.
- Goedert JL, Peckmann J and Reitner J (2000) Worm tubes in an allochthonous cold-seep carbonate from lower Oligocene rocks of western Washington. *Journal of Paleontology* **74**, 992–9.
- Goedert JL and Squires RL (1990) Eocene deep-sea communities in localized limestones formed by subduction-related methane seeps, southwestern Washington. *Geology* **18**, 1182–5.
- Goedert JL and Squires RL (1993) First Oligocene record of *Calyptogenia* (Bivalvia: Vesicomidae). *Veliger* **36**, 72–7.
- Goedert JL, Thiel V, Schmale O, Rau WW, Michaelis W and Peckmann J (2003) The Late Eocene ‘Whiskey Creek’ methane-seep deposit (western Washington State). Part I: Geology, palaeontology, and molecular geobiology. *Facies* **48**, 223–40.

- Greenstein BJ (1991) An integrated study of echinoid taphonomy: predictions for the fossil record of four echinoid families. *Palaios* 6, 519–40.
- Hinrichs K-U, Hayes JM, Sylva SP, Brewer PG and DeLong EF (1999) Methane-consuming archaeobacteria in marine sediments. *Nature* 398, 802–5.
- Hovland, M, Talbot MR, Qvale H, Olausen S and Aasberg L (1987) Methane-related carbonate cements in pockmarks. *Journal of Sedimentary Petrology* 57, 881–92.
- Hryniewicz K, Amano K, Jenkins R and Kiel S (2017) Thyasirid bivalves from Cretaceous and Paleogene cold seeps. *Acta Palaeontologica Polonia* 62, 705–28.
- Hryniewicz K (2022a) Ancient seep carbonates: from outcrop appearance to microscopic petrography. In *Ancient Hydrocarbon Seeps* (eds A Kaim, JK Cochran and NH Landman), pp. 79–110. *Topics in Geobiology* 53. Cham: Springer.
- Hryniewicz K (2022b) Ancient hydrocarbon seeps of the world. In *Ancient Hydrocarbon Seeps* (eds A Kaim, JK Cochran and NH Landman), pp. 571–647. *Topics in Geobiology* 53. Cham: Springer.
- Hybertsen F and Kiel S (2018) A middle Eocene seep deposit with silicified fauna from the Humptulips Formation in western Washington State, USA. *Acta Palaeontologica Polonica* 63, 751–68.
- Jakubowicz M, Kiel S, Goedert JL, Dopieralska J and Belka Z (2020) Fluid expulsion system and tectonic architecture of the incipient Cascadia convergent margin as revealed by Nd, Sr and stable isotope composition of mid-Eocene methane seep carbonates. *Chemical Geology* 558, 119872.
- Joye SB (2020) The geology and biogeochemistry of hydrocarbon seeps. *Annual Review of Earth and Planetary Sciences* 48, 205–31
- Kato M, Oji T and Shirai K (2017) Paleoecology of echinoderms in cold seep environments revealed by isotope analysis in the late Cretaceous western interior seaway. *Palaios* 32, 218–30.
- Kiel S (2006) New records and species of molluscs from Tertiary cold-seep carbonates in Washington State, USA. *Journal of Paleontology* 80, 121–37.
- Kiel S (2010) An Eldorado for paleontologists: the Cenozoic seeps of western Washington State, USA. In *The Vent and Seep Biota* (ed S Kiel), pp. 433–48. *Topics in Geobiology* 33. Dordrecht: Springer Science+Business Media.
- Kiel S and Amano K (2013) The earliest bathymodiolin mussels: evaluation of Eocene and Oligocene taxa from deep-sea methane seep deposits in western Washington State, USA. *Journal of Paleontology* 87, 589–602.
- Kiel S and Peckmann J (2007) Chemosymbiotic bivalves and stable carbon isotopes indicate hydrocarbon seepage at four unusual Cenozoic fossil localities. *Lethaia* 40, 345–57.
- Kier PM (1977) The poor fossil record of the regular echinoid. *Palaeobiology* 3, 168–74.
- Kroh A, Lukeneder A and Gallemi J (2014) *Absurdaster*, a new genus of basal atelostomate from the Early Cretaceous of Europe and its phylogenetic position. *Cretaceous Research* 48, 235–49.
- Kuechler RR, Birgel D, Kiel S, Freiwald A, Goedert JL, Thiel V and Peckmann J (2012) Miocene methane-derived carbonates from south-western Washington, USA and a model for silicification at seeps. *Lethaia* 45, 259–73.
- Lessard-Pilon SA, Porter MD, Cordes EE, MacDonald I and Fisher CR (2010) Community composition and temporal change at deep Gulf of Mexico cold seeps. *Deep-Sea Research Part II* 57, 1891–1903.
- Moore JC and Vrolijk P (1992) Fluids in accretionary prisms. *Reviews of Geophysics* 30, 113–35.
- Mortensen T (1950) New Echinoidea (Spatangoida). *Videnskabelige Meddelelser fra Dansk Naturhistorisk Forening* 112, 156–63.
- Nesbitt EA, Martin RA and Campbell, CA (2013) New records of Oligocene diffuse hydrocarbon seeps, northern Cascadia margin. *Palaeogeography, Palaeoclimatology, Palaeoecology* 390, 116–29.
- Niem AR, Snaveley PD Jr, Chen Y and Niem WA (1989) Jansen Creek Member of the Makah Formation: a major Oligocene submarine landslide or slump deposit from the Vancouver Shelf in the Juan de Fuca deep marginal basin, northwest Olympic Peninsula, Washington. *Geological Society of America Abstracts with Programs* 21, 123.
- Niemann H and Elvert M (2008) Diagnostic lipid biomarker and stable carbon isotope signatures of microbial communities mediating the anaerobic oxidation of methane with sulphate. *Organic Geochemistry* 39, 1668–77.
- Olu K, Sibuet M, Fiala-Médioni A, Gofas S, Salas C, Mariotti A, Foucher J-P and Woodside J (2004) Cold seep communities in the deep eastern Mediterranean Sea: composition, symbiosis and spatial distribution on mud volcanoes. *Deep-Sea Research Part I* 51, 1915–36.
- Paull CK, Hecker B, Commeau R, Freeman-Lynde RP, Neumann C, Corso WP, Golubic S, Hook JE, Sikes E and Curray J (1984) Biological communities at the Florida Escarpment resemble hydrothermal vent taxa. *Science* 226, 965–7.
- Pawson DL, Nizinski MS, Ames CL and Pawson DJ (2015) Deep-sea echinoids and holothurians (Echinodermata) near cold seeps and coral communities in the northern Gulf of Mexico. *Bulletin of Marine Science* 91, 167–204.
- Peckmann J, Birgel D and Kiel S (2009) Molecular fossils reveal fluid composition and flow intensity at a Cretaceous seep. *Geology* 37, 847–50.
- Peckmann J, Gischler E, Oschmann W and Reitner J (2001) An Early Carboniferous seep community and hydrocarbon-derived carbonates from the Harz Mountains, Germany. *Geology* 29, 271–4.
- Peckmann J, Goedert JL, Heinrichs T, Hoefs J and Reitner J (2003) The Late Eocene ‘Whiskey Creek’ methane-seep deposit (western Washington State). Part II: Petrology, stable isotopes, and biogeochemistry. *Facies* 48, 241–54.
- Peckmann J, Goedert JL, Thiel V, Michaelis W and Reitner J (2002) A comprehensive approach to the study of methane-seep deposits from the Lincoln Creek Formation, western Washington State, USA. *Sedimentology* 49, 855–73.
- Peckmann J, Senowbari-Daryan B, Birgel D and Goedert JL (2007) The crustacean ichnofossil *Palaxius* associated with callianassid body fossils in an Eocene methane-seep limestone, Humptulips Formation, Olympic Peninsula, Washington. *Lethaia* 40, 273–80.
- Peckmann J and Thiel V (2004) Carbon cycling at ancient methane-seeps. *Chemical Geology* 205, 443–67.
- Peckmann J, Thiel V, Michaelis W, Clari P, Gaillard C, Martire L and Reitner J (1999) Cold seep deposits of Beauvoisin (Oxfordian; southeastern France) and Marmorito (Miocene, northern Italy): microbially induced authigenic carbonates. *International Journal of Earth Sciences* 88, 60–75.
- Prothero DR, Draus E and Burns C (2009) Magnetostratigraphy and tectonic rotation of the Eocene-Oligocene Makah and Hoko River formations, northwest Washington, USA. *International Journal of Geophysics* 2009, 930612.
- Riedel B, Zuschin M, Haselmair A and Stachowitsch M (2008) Oxygen depletion under glass: behavioural responses of benthic macrofauna to induced anoxia in the Northern Adriatic. *Journal of Experimental Marine Biology and Ecology* 367, 17–27.
- Ritger S, Carson S and Suess E (1987) Methane-derived authigenic carbonates formed by subduction-induced pore-water expulsion along the Oregon/Washington margin. *Geological Society of America Bulletin* 98, 147–56.
- Rybakova E, Krylova EM, Mordukhovich V, Galkin SV, Alalykina I, Smirnov I, Sanamyan N, Nekhaev I, Vinogradov G, Shilov V, Prudkovsky A, Kolpakov E, Gebruk AV and Adrianov A (2022) Methane seep communities on the Koryak slope in the Bering Sea. *Deep-Sea Research II* 206, 105203.
- Sahling H, Rickert D, Lee RW, Linke P and Suess E (2002) Macrofaunal community structure and sulfide flux at gas hydrate deposits from the Cascadia convergent margin, NE Pacific. *Marine Ecology Progress Series* 231, 121–38.
- Savard M (1996) Significance of aragonite cements around Cretaceous marine methane seeps. *Journal of Sedimentary Research* 66, 430–8.
- Schlüter N, Wiese F and Reich M (2015) Systematic assessment of the Atelostomata (Spatangoida and Holasteroidea; irregular echinoids) based on spine microstructure. *Zoological Journal of the Linnean Society* 175, 510–24.
- Scholz F, Hensen C, Schmidt M and Geersen J (2013) Submarine weathering of silicate minerals and the extent of pore water freshening at active continental margins. *Geochimica et Cosmochimica Acta* 100, 200–16.
- Sibuet M and Olu K (1998) Biogeography, biodiversity and fluid dependence of deep-sea cold-seep communities at active and passive margins. *Deep-Sea Research Part II* 45, 517–67.
- Smith AB (1984) *Echinoid Palaeobiology*. London: Allen & Unwin, 192 pp.
- Smrzka D, Kraemer SM, Zwicker J, Birgel D, Fischer D, Kasten S, Goedert JL and Peckmann J (2015) Constraining silica diagenesis in methane-seep deposits. *Palaeogeography, Palaeoclimatology, Palaeoecology* 420, 13–26.

- Smrzka D, Zwicker J, Kolonic S, Birgel D, Little CTS, Marzouk AM, Chellai EH, Wagner T and Peckmann J** (2017) Methane seepage in a Cretaceous greenhouse world recorded by an unusual carbonate deposit from the Tarfaya Basin, Morocco. *The Depositional Record* **3**, 4–37.
- Snively PD Jr, MacLeod NS and Niem AR** (1993) Geologic map of the Cape Flattery, Clallam Bay, Ozette Lake, and Lake Pleasant quadrangles, northwestern Olympic Peninsula, Washington. *US Geological Survey Miscellaneous Investigations Series Map I-1946*, scale 1:48,000.
- Snively PD Jr, Niem AR, MacLeod NS, Pearl JE and Rau WW** (1980) Makah Formation: a deep-marginal-basin sedimentary sequence of Late Eocene and Oligocene age in the northwestern Olympic Peninsula, Washington. *US Geological Survey Professional Paper* 1162 B, 1–28.
- Snively PD Jr and Wells R** (1996) Cenozoic evolution of the continental margin of Oregon and Washington. In *Assessing Earthquake Hazards and Reducing Risk in the Pacific Northwest* (eds TJ Walsh, WJ Kockelman and GR Priest). *US Geological Survey Professional Paper* 1560, **1**, 161–82.
- Squires RL** (1995) First fossil species of the chemosynthetic-community gastropod *Provanna*: localized cold-seep limestones in upper Eocene and Oligocene rocks, Washington. *Veliger* **38**, 30–6.
- Stewart RJ and Brandon MT** (2004) Detrital-zircon fission-track ages for the “Hoh Formation”: implications for late Cenozoic evolution of the Cascadia subduction wedge. *Bulletin of the Geological Society of America* **116**, 60–75.
- Tabor RW and Cady WM** (1978) Geologic map of the Olympic Peninsula, Washington. *US Geological Survey Miscellaneous Investigations Series Map I-994*, scale 1:125,000.
- Thiel V, Peckmann J, Seifert R, Wehrung P, Reitner J and Michaelis W** (1999) Highly isotopically depleted isoprenoids: molecular markers for ancient methane venting. *Geochimica et Cosmochimica Acta* **63**, 3959–66.
- Van Dover CL, Aharon P, Bernhard JM, Caylor E, Doerries M, Flickinger W, Gilhooly W, Goffredi SK, Knick KE, Macko SA, Rapoport S, Raulfs EC, Ruppel C, Salerno JL, Seitz RD; Sen Gupta BK, Shank T, Turnipseed M and Vrijenhoek R** (2003) Blake Ridge methane seeps: characterization of a soft-sediment, chemosynthetically based ecosystem. *Deep-Sea Research Part I* **50**, 281–300.
- Wells R, Bukry D, Friedman R, Pyle D, Duncan R, Haeussler P and Wooden J** (2014) Geologic history of Siletzia, a large igneous province in the Oregon and Washington Coast Range: correlation to the geomagnetic polarity time scale and implications for a long-lived Yellowstone hotspot. *Geosphere* **10**, 692–719.
- Yao H, Panieri G, Lehmann MF, Himmler T and Niemann H** (2021) Biomarker and isotopic composition of seep carbonates record environmental conditions in two arctic methane seeps. *Frontiers in Earth Science* **8**, Article 570742, 1–12.
- Zwicker J, Smrzka D, Gier S, Goedert JL and Peckmann J** (2015) Mineralized conduits are part of the uppermost plumbing system of Oligocene methane-seep deposits, Washington State (USA). *Marine and Petroleum Geology* **66**, 616–30.